Study of a monocrystalline Cu-Al-Ni shape memory alloy by infrared thermography

C. BUBULINCĂ[a,b], X. BALANDRAUD[a], D. DELPUEYO[a], M. GREDIAC[a], S. STANCIU[c], M. ABRUDEANU[b*], A.-G. PLAIASU[b*], M. M. DICU[b], E. L. NITU[b]
[a]*Clermont University, Blaise Pascal University, IFMA, Institut Pascal UMR CNRS 6602, BP 10448, 63000 Clermont-Ferrand, France*
[b]*University of Pitesti, Targu din Vale, No 1, 110040, Pitesti, Romania*
[c]*Tehnical University Gh. Asachi of Iasi, Bd. D. Mangeron 61A, 700050 Iasi, Romania*

In this article we study a monocrystalline Cu-Al-Ni shape memory alloy subjected to a small periodic tensile loading at ambient temperature. An infrared camera is used to capture the temperature fields at the specimen surface. As a result of the small loading oscillation, very localized thermal activities are observed. The heterogeneity of the temperature oscillation at the specimen surface is studied. Austenite-martensite interfaces are revealed by the thermal field processing.

(Received November 23, 2012; accepted June 12, 2013)

Keywords: Shape memory alloy, Thermomechanical analysis, Infrared thermography

1. Introduction

Shape memory alloys (or SMA) are a special class of metallic alloys with peculiar mechanical properties such as pseudoelasticity and shape memory effect. These macroscopic properties are due to a solid-to-solid phase transformation which is governed by temperature or stress changes [1]. The present study focuses on the stress-induced phase transformation. The phase change is accompanied by latent heat production or absorption. The austenite-to-martensite transformation is exothermic while the inverse transformation is endothermic. The idea is here to analyze the microstructure changes in a SMA specimen subjected to mechanical loading at constant ambient temperature by tracking the temperature changes at the specimen surface. An infrared camera was use for this purpose. Tests were performed on a Cu-Al-Ni single crystal as the martensitic microstructures were expected to grow at the macroscopic level in this case, while in case of polycrystals, the microstructures would be localized in small grains.

During a stress-induced phase transformation at ambient temperature, thermomechanical couplings play an important role in the macroscopic mechanical response. During the austenite-to-martensite change, the production of latent heat contributes to an overall increase of sample temperature, and this change in temperature influences the kinetics of transformation. The link between temperature change and transformation kinetics was studied in details in several references [2-7]. It can be noted that, in addition of this thermomechanical coupling related to phase transformation, a thermoelastic coupling also participates to the temperature variation, as in all materials. This second type of coupling is directly connected to the value of the coefficient of thermal expansion of the material. In case of a cyclic mechanical loading, the thermoelastic coupling is at the base of the so-called Thermoelastic Stress Analysis, which is used to measure the field of stress amplitude in a structure [8]. A few applications were done on SMA [9].

The understanding of the spatial organization of the phases within a SMA specimen is of great interest as the martensitic microstructures are a key element influencing the macroscopic behavior of the material. Classic means such as microscopes are widely used to observe and analyze the microstructures. Full-field measurement techniques are also available. Optical images can be used to measure strain fields by digital image correlation [10] or by the grid method [11] Thermal images can be also used. In this case, the data processing consists in extracting heat sources from the temperature maps, or in analyzing the temperature oscillation when the mechanical loading is cyclic.

The objective here is to identify austenite-martensite interfaces using infrared thermography. Section 2 presents the experimental setup. Section 3 presents preliminary information about the macroscopic stress-strain curve. Section 4 presents the results obtained following a specific mechanical loading enabling us to reveal the interfaces between austenite and martensite.

2. Experimental setup

2.1. Material and specimen

The specimen is a Cu-Al-Ni single crystal provided by Nimesis Technology (Metz, France). It is a flat wire with dimensions $0.92\times2.88\times100$ mm^3 along the x-, y- and z-directions, respectively (see Fig 1-a). The austenite-start temperature is about -90°C, so it is entirely austenitic at ambient temperature. Once the specimen was placed in the

jaws of the testing machine, the length of the gauge extion along z-direction was equal to 55 mm.

2.2. Experimental setup

2.2.1. Mechanical loading

Tests were performed using a uniaxial testing machine MTS ±15kN. The following loading procedure was applied (see Fig. 1-b):

- Stage 1: the specimen was partially transformed to martensite, up to a macroscopic strain which is denoted ε_{macro} in the following;
- Stage 2: a waiting period was imposed to allow the specimen to return to room temperature. Indeed, during the previous stage, the temperature of the specimen increased due to the latent heat associated with the austenite-to-martensite phase change. The duration was of three minutes in practice.
- Stage 3: a small periodic macroscopic strain was imposed to the specimen. In the following, the loading frequency, the duration and the amplitude of the strain oscillation are denoted by f_L, T_L and $\Delta\varepsilon_{macro}$, respectively.

The higher the loading frequency during Stage 3, the better the local adiabaticity under cyclic loading. After some preliminary tests which are not reported here, a frequency f_L of 13 Hz was chosen for all the tests. The duration T_L of the cyclic loading was short for all the tests in order to limit damage due to fatigue: 10 seconds were used in practice. The macroscopic strain ε_{macro} was fixed to 2.73% Nine values of $\Delta\varepsilon_{macro}$ were tested: ±0.018%, ±0.026%, ±0.054%, ±0.073%, ±0.091%, ±0.136%, ±0.182%, ±0.227% and ±0.273%.

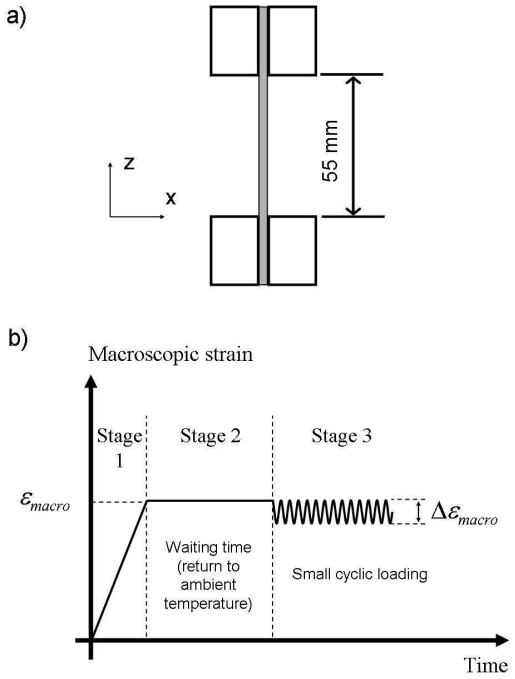

Fig. 1. a) Specimen and useful length. b) Scheme of the loading procedure.

2.2.2. Temperature measurement

A Cedip Jade III-MWIR infrared camera was used during Stage 3 to capture the temperature fields at the specimen surface. Integration time was set to 1500 μs. The acquisition frequency f_a was set to 150 Hz. This frequency was chosen as a non-multiple of the loading frequency f_L for a better data treatment by discrete Fourier transformation. The spatial resolution (size of the pixel on the specimen surface) was equal to 0.24 mm. We have then about eleven pixel along the width of the specimen. Prior to tests, the specimen was painted in black in order to obtain a thermal emissivity close to one. The thermal resolution was about 0.02 C.

2.3. Data processing

2.3.1. Heat sources

In a SMA specimen subjected to mechanical loading, the total heat source (in W/m^3) produced by the material due to the strain change can be divided into three quantities:

- a heat source s_{ther} due the thermoelastic coupling. corresponding to the coupling between temperature and the elastic strain in the free energy expression. Its expression is given for an isotropic material by:

$$s_{ther} = -\alpha T \, \mathrm{d}\sigma / \mathrm{d}t \qquad (1)$$

where α is the coefficient of thermal expansion, T the temperature in Kelvin (it is then nearly constant in this equation for a temperature change of a few degrees), and σ the sum of the principal stresses (it is equal to the longitudinal stress for the present uniaxial tests). This heat source is negative when the stress increases, and positive when the stress decreases;

- a heat source s_{transf} due to phase change. It is positive for an austenite-to-martensite transformation and negative for the inverse transformation;

- a heat source d_1 corresponding to intrinsic dissipation. It is related to mechanical irreversibilities such as fatigue, plasticity, etc. This quantity is always positive.

2.3.2. Application to Stage 3

The thermal signal which is recorded during the cyclic stage of the loading procedure (Stage 3) is expected to provide information about the microstructure changes. Indeed, the cyclic loading is expected to lead to a cyclic movement of the austenite-martensite interfaces. Let us discuss on the effects of the three heat source terms presented above:

- due to thermoelastic coupling, the temperature oscillates in opposite phase with the load. If the loading frequency is high enough, the amplitude ΔT_{therm} of the

temperature oscillation due to thermoelastic coupling is proportional to the amplitude $\Delta\sigma$ of the stress oscillation:

$$\Delta T_{therm} = \alpha T_0 \Delta\sigma \quad (2)$$

where T_0 is the mean temperature (in Kelvin);

- due to phase transformation, the temperature oscillates in phase with the load, as a consequence of the austenite↔martensite cyclic transformation. Let us denote by ΔT_{transf} the temperature oscillation due to the phase transformation. In purely austenitic zones and in purely martensitic zones, this effect is not present: $\Delta T_{transf} = 0$. It is expected to appear along the austenite-martensite interfaces: $\Delta T_{transf} \neq 0$. If the amplitude of the cyclic loading is small, we have then the possibility to localize the austenite-martensite interfaces;

- due to intrinsic dissipation, the temperature increases. It generally stabilizes as a consequence of an equilibrium between the heat which is produced and the heat which is exchanged with the outside of the specimen.

As the amplitude of the cyclic loading is small, the effect of the thermoelastic coupling is small. So we have $\Delta T_{therm} << \Delta T_{transf}$.

2.3.3. Extraction of the amplitude ΔT of the temperature oscillation

Let us denote by ΔT (x, z) the amplitude of the temperature oscillation for each material point of the specimen surface, at where x and z are the pixel coordinates.

$$\Delta T = \Delta T_{therm} + \Delta T_{transf} \approx \Delta T_{transf}. \quad (3)$$

A Fourier analysis was performed during Stage 3. In practice, the amplitude ΔT of the oscillation in temperature was calculated for each pixel of the specimen surface.

3. Preliminary information: macroscopic strain-stress curve

Figure 2 presents the macroscopic stress-strain curve. Classically, Stage 1 is characterized first by an elastic response of the austenite specimen, second by a progressive transformation to martensite. This second step starts for a stress of 180 MPa. The stress then slightly increases. During Stage 2, the stress slightly decreases. This is due to a continuation of the phase transformation resulting from the return to ambient temperature [12] . Indeed, temperature increased during the previous stage due to a production of latent heat. During Stage 3 (cyclic loading), the response is globally elastic, with small hysteresis loop if any. This hysteresis increases with the value of $\Delta\varepsilon_{macro}$.

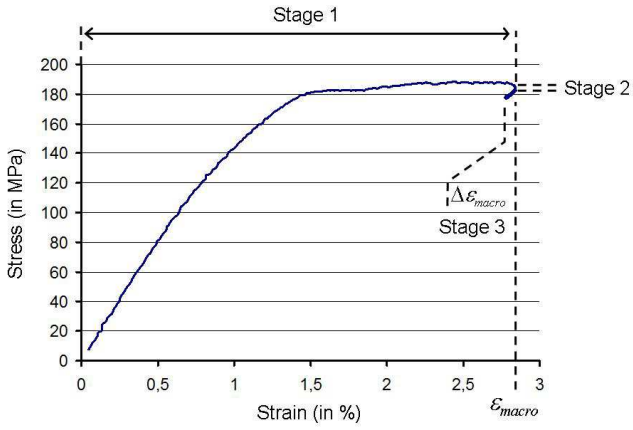

Fig. 2. Macroscopic stress-strain curve.

4. Results during the cyclic loading

Section 4.1 presents a typical result (for $\Delta\varepsilon_{macro}$ = ±0.026%). Section 4.2 presents a comparison between the different tests in order to analyze the influence of $\Delta\varepsilon_{macro}$.

4.1. Typical result

Figure 3 presents the field ΔT for $\Delta\varepsilon_{macro}$ = ±0.026%. A strong thermal activity is observed in some zones. Six peaks are identified. The zones of strong thermal activity are perpendicular to the loading axis. This orientation probably results from the austenite crystal orientation with respect to the loading direction. Figure 4 proposes an interpretation in terms of microstructures. Each peak can be interpreted as an interface between austenite and martensite, whose cyclic movement leads to a temperature oscillation due to a cyclic production-absorption of latent heat.

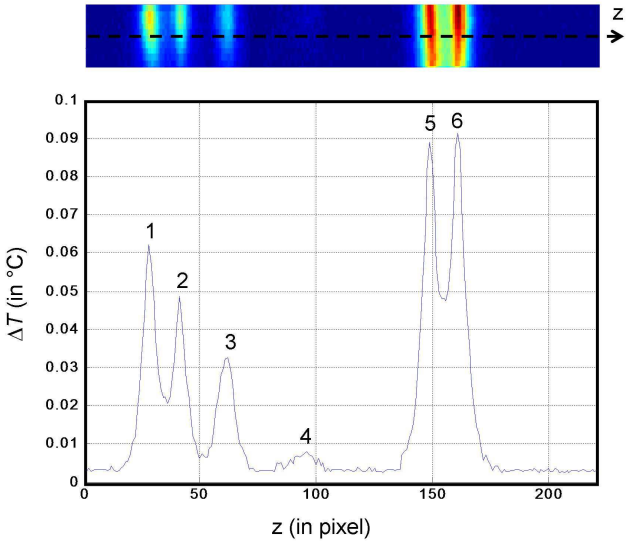

Fig. 3. Results for $\Delta\varepsilon_{macro}$ = ±0.026%.

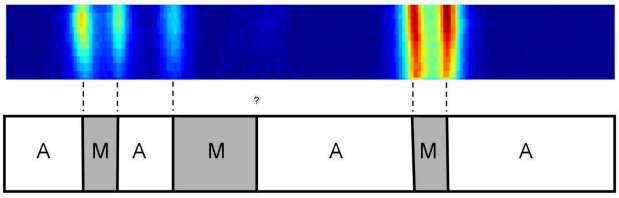

Fig. 4. Interpretation in terms of microstructures. A=austenite, M=martensite.

The six peaks have different intensities in terms of thermal activity. The higher activity is observed for peaks 5 and 6, meaning that the two interfaces have the largest amplitude of oscillation during the cyclic loading. On the contrary, the lowest thermal activity is observed on peak 4, making difficult the localization of the corresponding interface. It can be noted that the peaks have a certain width. This width can be related to the amplitude of the oscillation of the interface, but it can be guessed that it is also related to heat conduction (non-perfect local adiabaticity).

4.2. Influence of $\Delta\varepsilon_{macro}$

Figures 5, 6 and 7 show the maps of ΔT for the other eight values of $\Delta\varepsilon_{macro}$ which were tested. It can be observed that the thermal intensity varies as a function of $\Delta\varepsilon_{macro}$:

- let us first analyze the maximum value to ΔT: see Table 1. We see that the value increases with $\Delta\varepsilon_{macro}$ (except for ±0.227%). This is logical as the strain amplitude is directly related to the quantity of material which is subjected to a cyclic austenite↔martensite transformation.

$\Delta\varepsilon_{macro}$	max ΔT
±0.018%	0.035
±0.026%	0.091
±0.054%	0.150
±0.073%	0.207
±0.091%	0.430
±0.136%	0.801
±0.182%	1.320
±0.227%	1.121
±0.273%	2.430

Table 1. Maximum value of the temperature oscillation amplitude ΔT as a function of strain amplitude $\Delta\varepsilon_{macro}$.

- when we analyze the distribution of the thermal activities in the specimen, it can be noted that all maps share some common features for the six lowest values of $\Delta\varepsilon_{macro}$ (±0.018%, ±0.026%, ±0.054%, ±0.073%, ±0.091%, and ±0.136%): six peaks are observed. For the three highest values of $\Delta\varepsilon_{macro}$ (±0.182%, ±0.227% and ±0.273%), a different pattern of thermal activity is observed. In particular, some big peaks which were observed for the lowest values of $\Delta\varepsilon_{macro}$ are now much smaller, making difficult the microstructure identification.

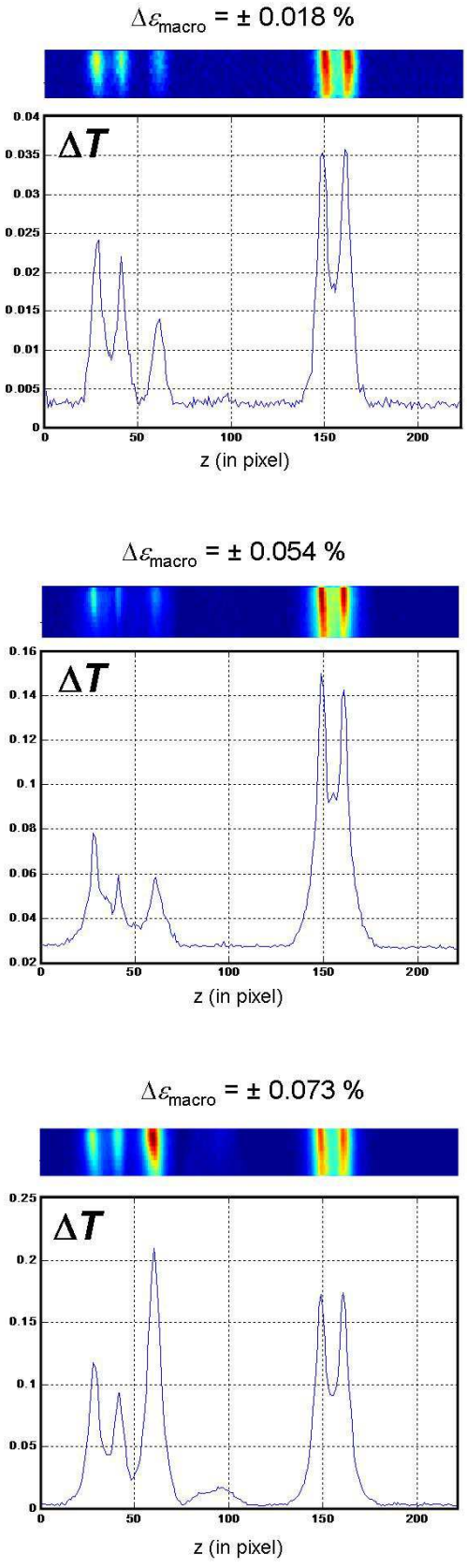

Fig. 5. Thermal activity for $\Delta\varepsilon_{macro}$ equal to ±0.018%, ±0.054% and ±0.073%.

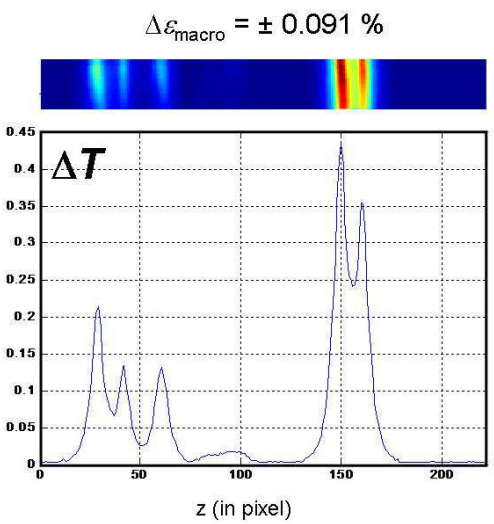

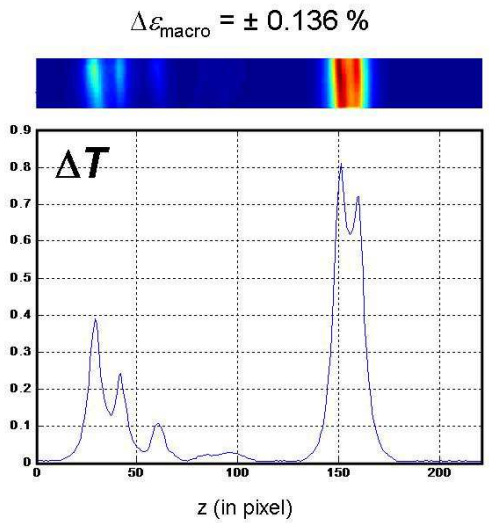

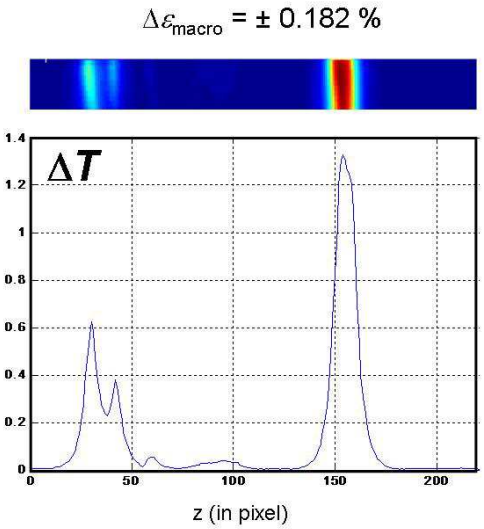

Fig.6. Thermal activity for $\Delta\varepsilon_{macro}$ equal to ±0.091%, ±0.136% and ±0.182%.

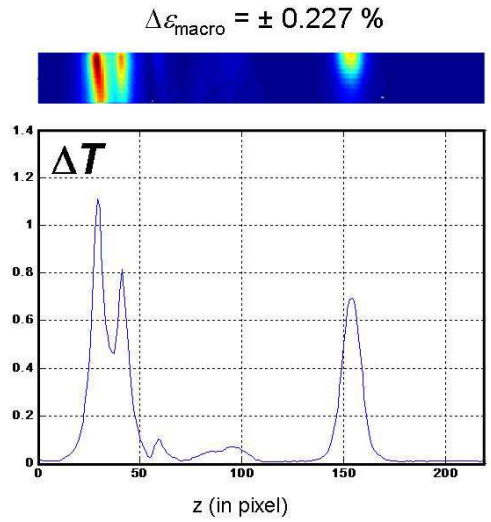

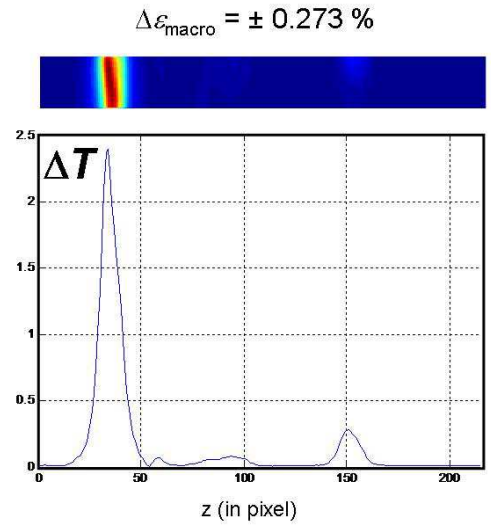

Fig.7. Thermal activity for $\Delta\varepsilon_{macro}$ equal to ±0.227% and ±0.273%.

5. Conclusion

We have studied the thermal response of a monocrystalline Cu-Al-Ni shape memory alloy subjected to periodic tensile loading at ambient temperature. As amplitudes of the load oscillation were small, very localized thermal activity was detected in the specimen. This thermal activity has been used to identify the location of austenite-martensite interfaces. It was noted that the identification becomes difficult if the amplitude of load oscillation increases too much.

The tested specimen was mainly unidimensional (a flat wire). The application to a two-dimensional shape memory alloy (a sheet) was performed in Reference [13], in which in addition the thermoelastic coupling was considered to extract complementary information from the temperature measurements.

References

[1] K. Bhattacharya. Microstructure of martensite: why it forms and how it gives rise to the shape memory effect. Oxford: Oxford University Press (2003)
[2] J.A. Shaw, S. Kyriakides, J. Mech. Phys. Solids **43**, 1243 (1995)
[3] J.A. Shaw, S. Kyriakides, Acta Mater. **45**, 683 (1997)
[4] R. Peyroux, A. Chrysochoos, C. Licht, M. Löbel, Int. J. Eng. Sci. **36** , 489 (1998)
[5] X. Balandraud, A. Chrysochoos, S. Leclercq, R. Peyroux, C. R. Acad. Sci., Ser. IIb: Mec. **329**(8), 621 (2001)
[6] B. Vieille, J.F. Michel, M.L. Boubakar, C. Lexcellent, Int. J. Mech. Sci. **49**, 280 (2007)
[7] X. Balandraud, E. Ernst, E. Soos, C. R. Acad. Sci., Ser. IIb: Mec. **327** (1), 33 (1999)
[8] J.M. Dulieu-Barton, P. Stanley, J. Strain Anal. Eng. Design **33**, 93 (1998)
[9] J. Eaton-Evans, J.M. Dulieu-Barton, E.G. Little, I.A. Brown, J. Strain Anal. Eng. Design **41**, 481 (2006)
[10] C. Bewerse, K.R. Gall, G.J. McFarland, P. Zhu, L.C. Brinson, Mater. Sci. Eng. A **568**, 134 (2013)
[11] D. Delpueyo, M. Grediac, X. Balandraud, C. Badulescu, Mech. Mater. **45**, 34 (2012)
[12] X. Balandraud, E. Ernst, E. Soos, Zeit. Angew. Math. Phys. **51**(3), 419 (2000)
[13] D. Delpueyo, X. Balandraud, M. Grédiac, Mater. Sci. Eng. A **528**(28), 8249 (2011)

*Corresponding authors: gabriela.plaiasu@upit.ro, abrudeanu@upit.ro